Production of porous SiC by liquid phase sintering using graphite as sacrificial phase: influence of SiO_2 and graphite on the sintering mechanisms

C. Soto, C. García-Rosales *, J. Echeberria

Ceit-IK4 Technology Center, E-20018 San Sebastian, Spain and
Universidad de Navarra, Tecnun, E-20018 San Sebastian, Spain

Abstract

Porous silicon carbide (SiC) is a promising ceramic for high-temperature applications due to its unique combination of properties. In the present work, a fabrication route for porous SiC is presented using graphite spherical powder as sacrificial phase to introduce porosity. By varying the initial amount of sacrificial phase, high-performance SiC materials with porosities in the range 30-50% were manufactured and characterized in terms of microstructure, density, thermal conductivity and flexural strength. The materials were fabricated by liquid phase sintering in presence of 2.5 wt.% Al_2O_3 and Y_2O_3 as sintering additives. The results indicate that the SiO_2 present in the starting SiC powders interacts with the sintering additives forming liquid phases that promote densification and weight loss. Besides, an Al-Si liquid phase is formed at higher sintering temperatures, whose contribution to densification is inhibited in presence of graphite due to the formation of Al-rich carbides.

Keywords: silicon carbide, liquid phase sintering, thermal conductivity, sintering additives

1. Introduction

Silicon carbide (SiC) is a promising material for high-temperature applications as it exhibits an excellent stability against chemical agents and abrasion, a low expansion coefficient and high strength [1][2][3]. Due to the relatively high electrical and thermal conductivity of dense SiC [4], the development of porous SiC materials with insulating properties deserves special attention; diverse procedures to introduce porosity in SiC are described in the literature, being the most relevant ones those techniques based in partial sintering, the replica method, or the use of a sacrificial phase [5].

The highly covalent character of SiC makes it a material with very low sinterability, and Al_2O_3 and Y_2O_3 are often used as sintering additives in the production of SiC materials. The combination of Al_2O_3 and Y_2O_3 leads to the formation of liquid phases in which SiC is partially soluble; particularly, the addition of Al_2O_3 and Y_2O_3 in a 3:2 ratio give rise to a eutectic phase around 1800 °C, leading to the formation of YAG ($Y_3Al_5O_{12}$) and Al_2O_3 as intergranular phases. The use of liquid phase sintering allows the densification of the material at lower processing temperatures than by solid-state sintering, which are typically above 2000 °C [6].

The formation of liquid phases and their interaction with the SiC particles, however, increases the complexity of the system, making difficult to identify the phenomena governing the sintering [7]. Although this system has led to outstanding results in the production of SiC [8][9][10][11][12], a complete description of the sintering mechanisms still needs to be carried out, specially applied to the production of porous SiC. A special concern is the role of the SiO_2 always present at the surface of the SiC particles and its possible evaporation during sintering.

In the present work, a route for producing porous SiC by presureless sintering is presented, including 2.5 wt.% Al_2O_3-Y_2O_3 as sintering additives in a 3:2 weight relation. To introduce porosity, graphite spherical powder in form of mesocarbon microbeads (MCMB) is used as a sacrificial phase; after sintering, this phase is removed from the material by an oxidation treatment, producing spherical pores. The use as sacrificial phase of a graphite spherical powder with considerably higher particle size than the one of the SiC powder allows its easier removal after the sintering cycle, while the SiC particles densify around the spherical sacrificial particles creating a honeycomb-like porosity

* *Corresponding author: cgrosales@ceit.es*

distribution, which maximizes the strength of the material. The porosity of the final porous SiC materials as a function of the initial amount of sacrificial phase is presented, together with their microstructure, thermal conductivity and flexural strength. The material presented here was fabricated in the framework of the EUROfusion H2020 project, where materials for future nuclear fusion reactors are being developed. In the present case, SiC-based materials for application as isolating channels for a special type of breeding blanket in future fusion reactors were manufactured, for which these properties are particularly relevant [13][14][15][16]. To complete the study of the liquid phase sintering, the material is analyzed by EDS, DSC-TGA and X-ray diffraction. The influence of the SiO_2 content present in the starting SiC powders on the sintering mechanisms and densification process, as well as of the presence of graphite, is studied in detail and discussed. A more detailed reporting of these results and of the material's characterization can be found in [15].

2. Experimental procedure

As a first step in the production of porous SiC, a powder mixture was obtained including SiC powder (Superior Graphite, 0.3 μm), 1.5 wt.% of Al_2O_3 (Rio Tinto Alcan Inc., 0.4 μm), 1 wt.% of Y_2O_3 (HCST, 1 μm) and the sacrificial phase. The latter consist of a variable content of graphite spherical powder (mesocarbon microbeads, MCMB, Hebei ShunYe, ~18 μm), which was added to the initial mixture to introduce porosity.

To obtain optimum results in the liquid phase sintering of SiC, the sintering additives should be homogeneously distributed through the SiC powder [16]; the formation of agglomerates during the mixing step, commonly found due to the differences in surface potential of each powder and their reduced particle size, needs to be avoided [8]. To that effect, in the present work the mixing process was performed in two steps. A first long, high-energy step was applied, in order to adequately mix the sintering additives and the SiC powder; the graphite (MCMB) powder was then added in a shorter, gentler second mixing step, avoiding the fracture of the graphite spherical powder and preserving their spherical shape. Thus, the SiC powder and the additives were first mixed for 16-18 h in ethanol; Al_2O_3 mixing balls were added in this first step, together with 0.5 wt.% of Dolapix CE 64 (Zschmier & Schwartz) as a dispersing agent. The milling balls were then removed from the slurry, adding the MCMB. The slurry was blended for further 15 min., dried using a magnetic stirrer to avoid sedimentations, and finally meshed, obtaining a mixture with homogenous composition. 3 wt.% of Octapix AC112 (Zschmier & Schwartz) was used as a binder agent.

The powders were uniaxially pressed to the required geometries at 100 MPa. The green compacts were sintered in He atmosphere at two different conditions: 1850 °C for 1 h and 1900 °C for 30 min. To remove the sacrificial phase, the sintered samples were heated at 700 °C in air for 10 h.

The geometric density of the samples after sintering and after oxidation was measured from its weight and dimensions, determining their porosity by comparison between geometric and theoretical density, the latter obtained by the rule of mixtures. The microstructure was studied by field emission gun scanning electron microscopy (FESEM) and energy dispersive X-ray spectroscopy (EDS). The thermal conductivity as a function of temperature was determined from the thermal diffusivity, measured by the Laser Flash method (Netzsch LFA 457), the specific heat capacity and the geometric density. The flexural strength was measured at room temperature by three-point bending tests (3PBT) using at least 4 samples per condition, in an Instron 4505 using WC bolts and a velocity of the mobile crosshead of 0.2 mm/min. The dimensions of the samples were approximately 5x5x20 mm. The equipment used for the DSC-TGA analysis was a Setaram – Setsys Evolution 16/18; the analysis was limited to the reproduction of the first stage of the sintering, since the maximum operation temperature of the equipment was 1500 °C. The oxygen measurements were performed by the inert gas fusion method using a LECO TC 400 analyzer. X-ray diffraction (XRD) analysis was carried out with a PANalytical PW1700 diffractometer, comparing the results with the ICDD-cards database to identify the different phases.

3. Results

3.1 Characterization of porous SiC

By varying the initial amount of graphite sacrificial phase between 15 and 22 wt.%, porous SiC materials with a final porosity of ~30-50% were successfully fabricated. In Fig. 1, the final porosity of the materials is shown as a function of the initial MCMB for the two sintering conditions used. The results obtained for materials without sacrificial phase are also included. It can be observed that similar results are obtained with both sintering

conditions, with the exception of the samples produced without MCMB at 1850 °C, which present a significantly higher porosity after sintering compared to those produced at 1900 °C. In Fig. 2, the microstructure of some of the materials is shown, with spherical pores surrounded by the SiC matrix. In Fig. 3, high magnification images of the SiC matrix are compared in the case of sintering with and without sacrificial phase. The higher sintering grade of the SiC grains in the sample sintered without MCMB can be appreciated. The effect of sintering in presence of additional C will be discussed in next sections.

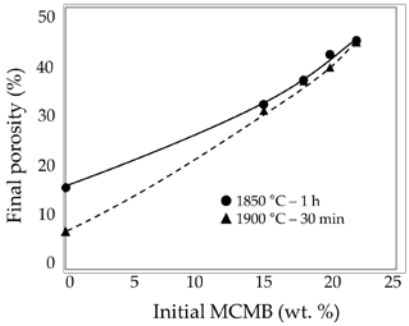

Fig. 1. Final porosity of the SiC materials as a function of the initial amount of MCMB sacrificial phase

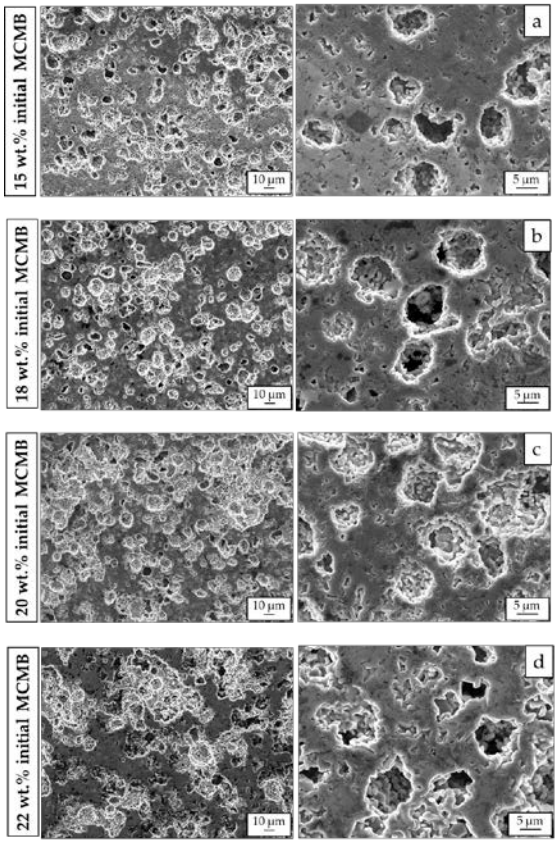

Fig. 2. Microstructure of the final porous SiC materials as a function of the initial amount of sacrificial phase (1850 °C for 1 h); a) 33% porosity; b) 40% porosity; c) 42% porosity; d) 48% porosity (FESEM, secondary electrons)

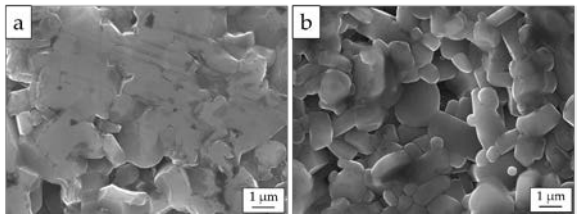

Fig. 3. Detail of the SiC matrix; a) 0% initial MCMB; b) 15% initial MCMB (1900 °C – 30 min) (FESEM, secondary electrons)

As mentioned in the introduction, the characterization of the materials was performed, focused on properties relevant for their application in isolating channels for a specific type of breeding blanket in a future nuclear fusion reactor. In Fig. 4, the thermal conductivity (k) of the materials as a function of porosity at three different temperatures (200, 500 and 700 °C) is presented. As expected, a decrease of thermal conductivity with increasing porosity and temperature is observed.

In Fig. 5, the flexural strength is presented. A nearly exponential decrease in strength with respect to the porosity is observed. The considerably high dispersion obtained in these measurements is attributed to the presence of defects in the samples, i.e. cracks derived from the uniaxial pressing step, due to difficulty of pressing hard powders with small particle size without provoking a high friction between the SiC powders and the pressing matrix. This suggest the convenience to adapting the production method to alternative routes avoiding uniaxial pressing to process the green samples. First results of the production of porous SiC using graphite as sacrificial phase by the gelcasting technique can be found in [13][17], a route that allows the future fabrication of larger ceramic parts with complex geometries. Despite the probable underestimation of the flexural strength due to the above-mentioned presence of defects in uniaxially pressed samples, the results obtained in this work are consistent with those reported by other authors in porous SiC materials fabricated by the sacrificial template method. In table 1, a comparison with similar materials is shown (the exact dispersion values are not provided by the authors). A wide review of the reported flexural strength of porous SiC materials as a function of the porosity can be consulted in [5], being the materials produced in this work in the high range of those fabricated by the sacrificial template method.

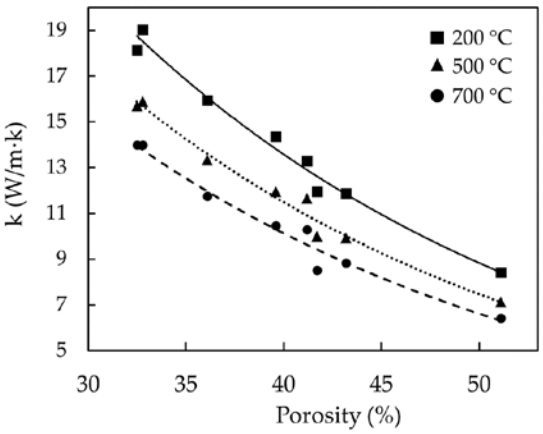

Fig. 4. Thermal conductivity of porous SiC as a function of porosity and temperature

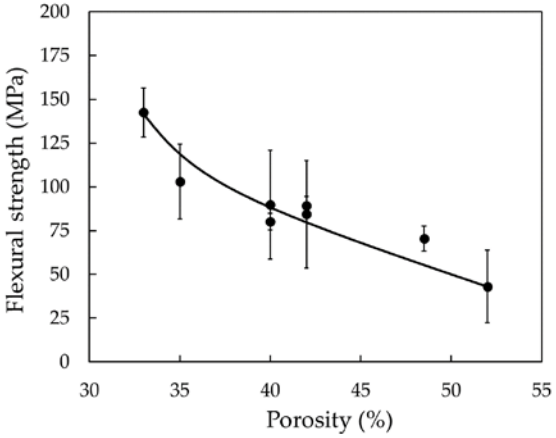

Fig. 5. Flexural strength of porous SiC as a function of the porosity

Table 1. Comparison of the flexural strength values obtained in this work with those reported in the literature for porous SiC materials

	Flexural strength (MPa)		
Porosity (%)	Eom et Kim [17]	Chae et al [18]	This work
~ 30	~ 105	~ 144	143 ± 14
~ 40	~ 75	~ 60	80 ± 5
~ 50	~ 40	~ 57	43 ± 21

The samples characterized were produced at two different sintering conditions studied (1850 °C – 1 h and 1900 °C – 30 min); since no significant influence of the sintering conditions was found in the results, no distinction is done in Figs. 3 and 4. As a summary, the properties of three porous SiC materials with different porosities are presented in table 2.

Table 2. Summary of properties of three porous SiC materials with different porosities

Initial MCMB (wt. %)	Porosity (%)	k (W/m·K)	Flexural strength (MPa)
15	~30	15	143 ± 14
18	~40	10	80 ± 5
20	~50	6.5	43 ± 21

3.2 Influence of the initial SiC powder

The microstructure and final density of the porous SiC materials produced by liquid phase sintering is strongly dependent on the starting SiC powder used. The influence of two main aspects can be highlighted: the predominant SiC polytype, and the particle size of the powder. If β-SiC (cubic) is used as the staring material, a β → α (hexagonal) polytypic transformation will take place during the coarsening stage of sintering, resulting in microstructures with highly elongated SiC grains. This transformation is also favored if a reduced amount of α-SiC is present in the initial mixture [19][20]. On the contrary, if α-SiC is the major phase in the initial SiC powder, materials with more equiaxed microstructures will be obtained [21][12]. In addition to the influence of the polytypes, the influence of the particle size of the starting SiC powders on the final results must be taken into account; smaller SiC particles have higher solubility in the liquid phases formed during sintering, often resulting in higher sintering rates for SiC powders with a higher specific surface area [10]. The particle size of the SiC powders usually correlates also with their SiO_2 content; a higher content tends to be found in fine powders due to their higher relative specific surface.

To determine the optimum starting material for the production of porous SiC with tailored porosity, several porous SiC materials were produced by the route previously described using three different SiC powders, whose characteristics are summarized in table 3 (all materials presented in section 2 were produced from powder number 3). To compare the influence of the three SiC starting powders on the densification achieved, the densities obtained after sintering in samples produced with 20 wt.% initial sacrificial phase are shown in table 4. All these samples were sintered at 1850 °C for 1 h.

Table 3. Initial SiC powders studied, all supplied by Superior Graphite

Name	Average particle size (μm)	Oxygen content (%)	SiC polytypes
1	0.6	1.8	β
2	0.5	3	β, α (6H)
3	0.3	3.4	α (6H, 4H), β

Table 4. Density and weight loss after the sintering of samples as a function of the initial SiC powder used (20 wt. % MCMB, 1850 °C – 1h)

	After sintering	
SiC powder	Weight loss (%)	Density (g/cm³)
1	6.8	2.04
2	7.7	2.09
3	9	2.29

The weight loss registered after sintering indicates that evaporation processes with associated gaseous products are taking place during the cycle; higher weight losses often correlate with lower relative densities, due to the additional porosity generated by the evaporation reactions. In the present work, however, the material manufactured from powder 3 presents a significantly higher density after sintering, despite exhibiting a considerable weight loss. The higher density obtained with this powder can be related to its predominantly hexagonal character or to its higher solubility in the liquid phases formed during sintering, due to the lower particle size. Besides, this powder corresponds to the finest SiC powder exhibiting the highest oxygen content; it can be thus assumed that it will have a higher SiO_2 content. A better densification of this powder due to the formation of SiO_2-derived liquid phases should be hence considered as well, being this aspect further discussed in the next section.

In table 5 the final density and porosity of the materials presented in table 4 after being subjected to the oxidation treatment to eliminate the MCMB sacrificial phase are presented. The higher final porosity of the materials fabricated from powders 1 and 2 is clearly pointed out, due to the additional porosity derived from the reduced densification during sintering. The final microstructure of the samples is shown in figure 6. The rest of materials discussed in this work were produced from powder 3.

Table 5. Final density and porosity of porous SiC samples as a function of the starting SiC powder (20 wt. % initial MCMB, sintering at 1850 °C – 1h, oxidation at 700 °C)

	After oxidation	
SiC powder	Density (g/cm³)	Porosity (%)
1	1.62	50
2	1.58	51
3	1.86	42

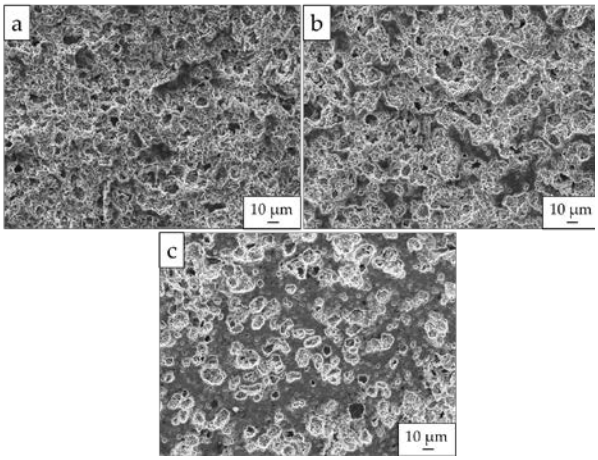

Fig. 6. Microstructure of the final porous SiC materials produced with a 20 wt.% initial MCMB, using as the initial SiC powder: a) Powder 1; b) Powder 2; c) Powder 3 (sintering at 1850 °C – 1h, oxidation at 700 °C)(secondary electrons)

4. Discussion

4.1 Interactions between SiO_2 and Al_2O_3-Y_2O_3

The higher weight loss of powder 3 after sintering suggest the elimination of the superficial SiO_2 during the heating ramp. A candidate explanation may be the SiO_2 evaporation due to its reaction with SiC [10]; this process, however, may be altered in presence of the sintering additives Al_2O_3 and Y_2O_3. In the literature, the formation of phases like YAG has been detected in samples sintered at temperatures <1500 °C [18], even if the Al_2O_3-Y_2O_3 phase diagram does not predict the formation of YAG until 1760 °C. A thermodynamic analysis of the SiO_2-Y_2O_3-Al_2O_3 systems performed by Can et al. [24] suggests the formation of liquid phases at lower sintering temperatures than the one predicted without taking into account the influence of SiO_2; this liquid phases result from interactions between SiO_2 and the sintering additives. The amount of liquid phase in the material during the heating ramp can be related to the initial SiO_2 content, which according to their calculations increases by a factor of 10 if the initial SiO_2 raises from 0.1 to 2 wt.%. If the

SiC particles are partially soluble in the melt formed, densification will be promoted, and the partial decomposition of SiC by these processes leads to a substantial weight loss after sintering.

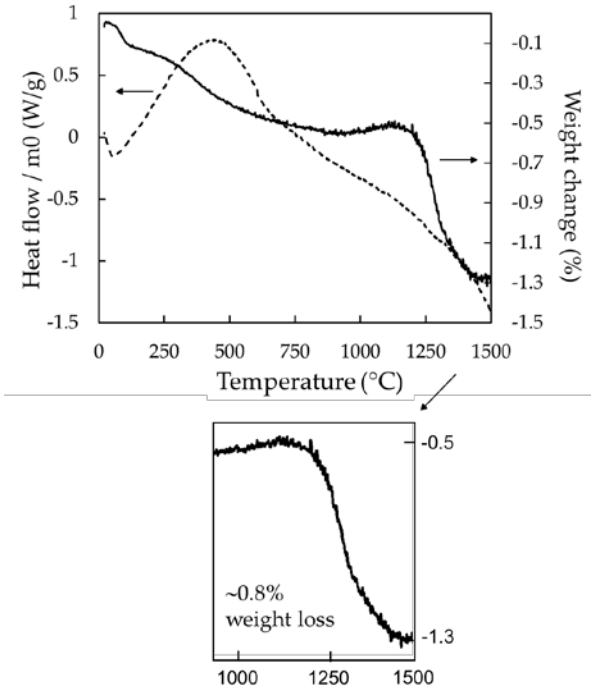

Fig. 7. DSC-TGA analysis of a sample of SiC powder 3. A detail of the weight loss registered at T > 1000 °C is shown

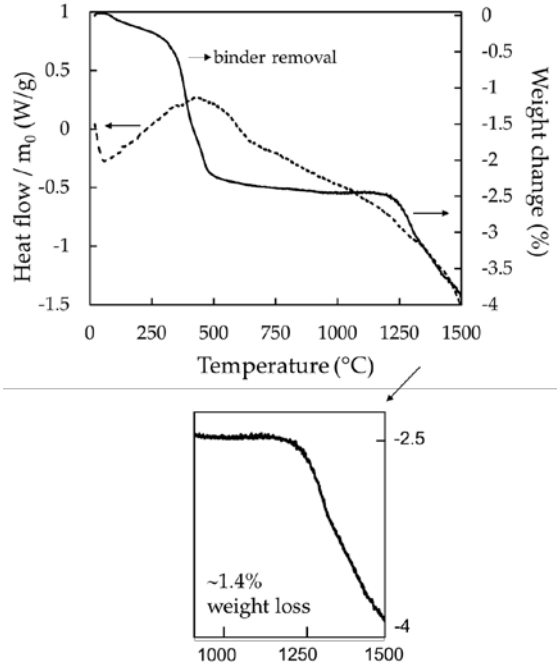

Fig. 8. DSC-TGA analysis of a sample of SiC powder 3, 2.5 wt.% Al_2O_3-Y_2O_3 and 2 wt.% organic binder. A detail of the weight loss registered at T > 1000 °C is shown

To obtain further information on the possible processes causing additional weight losses during sintering, the first stage of the sintering ramp was reproduced by DSC-TGA analysis. In figure 7, the results obtained on a sample from SiC powder 3 are shown. To address a possible interaction between the SiO_2 elimination and the sintering additives, these results are compared with those of a sample including SiC powder 3 and 2.5 wt.% sintering additives, shown in figure 8. This second sample also included 2 wt.% of organic binder; the first reaction causing weight loss is attributed to the binder burnout (arrow in Fig. 8).

A significant weight loss reaction is registered in both samples at >~1200 °C, pointing to the reduction of the SiO_2 layer. In the sample containing pure SiC, a 3.4 wt.% oxygen content was measured before the DSC-TGA cycle; after the test, the oxygen content was reduced down to 2.1 wt.%, supporting the assumption of a loss of SiO_2. A higher weight loss, however, was registered at the same temperature interval in the sample containing Al_2O_3-Y_2O_3, 1.4% vs 0.8%. This suggest the increase of SiO_2 elimination in samples sintered in presence of Al_2O_3-Y_2O_3. This result, together with the higher densification observed in samples sintered with a powder of higher SiO_2 content, supports the formation of liquid phases during the heating ramp that promote densification, as predicted by the thermodynamic calculations discussed above.

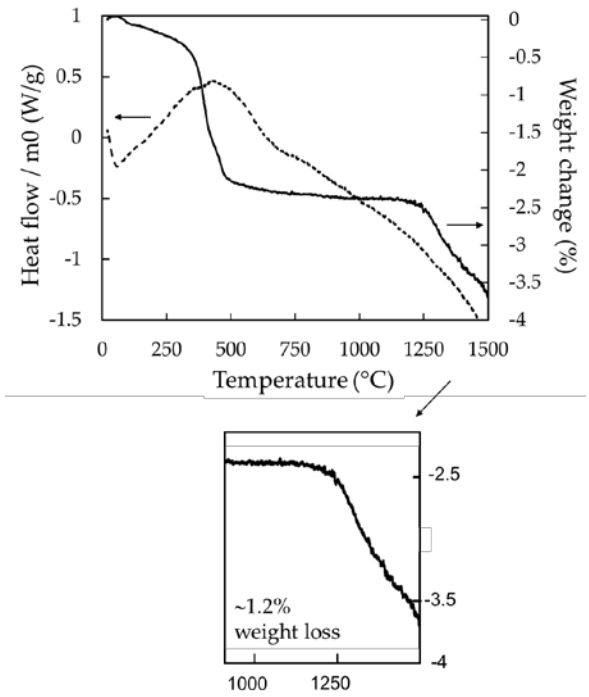

Fig. 9. DSC-TGA analysis of a sample of SiC powder 3, 2.5 wt.% Al_2O_3-Y_2O_3, 20 wt.% initial MCMB and 2 wt.% organic binder. A detail of the weight loss registered at T > 1000 °C is shown

To also address the possible influence of the MCMB (graphite sacrificial phase) on the above processes, the DSC-TGA analysis of a sample containing 20 wt.% initial MCMB is shown in figure 9. The results are similar to those presented in figure 8. However, the weight loss in the temperature range above 1200 °C is slightly reduced, suggesting the possible alteration or the partial inhibition of the SiO_2-Al_2O_3-Y_2O_3 interactions in presence of additional carbon. The influence of C will be further addressed in the next section.

4.2 Formation of Al-rich carbides

The fact that graphite is a high temperature phase allows performing the sintering in presence of the sacrificial phase; the SiC particles are thus able to densify surrounding the spherical particles, leading to spherical pores and resulting in a high strength, honeycomb-like microstructure. To perform the sintering in presence of high amounts of extra C, however, introduces an additional element that interacts with the sintering mechanisms. In the present work, a reduced densification was obtained in the samples sintered with MCMB if compared to those produced from pure SiC, as can be deduced from the results shown in figure 10 (results after sintering and before oxidation to remove the MCMB).

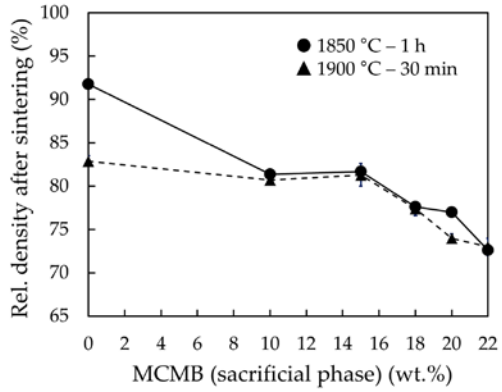

Fig. 10. Relative density after sintering (and before oxidation) as a function of the amount of initial MCMB

The liquid phase sintering of SiC in presence of additional carbon has been studied by other authors. The results obtained by Stobierski and Gubernat [25] pointed to a limitation of the mass transfer mechanisms associated to the SiO_2 decomposition due to carbon, hypothesis that is supported by the observations made in the DSC-TGA analysis of the present work. Accordingly, a limitation in the $\beta \rightarrow \alpha$ transformation and its related grain growth due to C was also reported, suggesting the relevance of the mass transport mechanisms in such a transformation; a similar effect was observed by Bereciartu et. al. [26].

Apart from the liquid phases originated from the SiO_2-Al_2O_3-Y_2O_3 interactions, the thermodynamic analysis of the system predict the formation of additional liquid phases at higher sintering temperatures [27][28][29]. The formation of an Al-Si metallic melt is predicted during the last stages of the heating ramp, due to the decomposition of SiC by Al_2O_3; since SiC is probably soluble in this liquid phase [27], a further densification of the material should be expected. In samples sintered in presence of additional C, however, the formation of the Al-Si melt is hindered by the formation of Al-C-Si mixed carbides [30][29]. Although in the calculations presented by Misra these interactions are predicted at temperatures near 1950 °C [27], the observations from other authors point to lower temperatures [12][31]; it should be taken into account that the presence of SiO_2 was not considered in Misra's calculations.

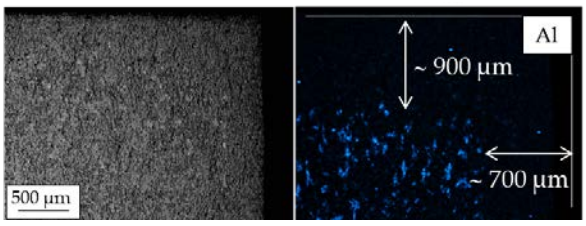

Fig. 11. EDS compositional map of the cross section of a sample sintered with 20 wt.% initial MCMB at 1850 °C for 1 h, where Al is highlighted in blue (primary electrons)

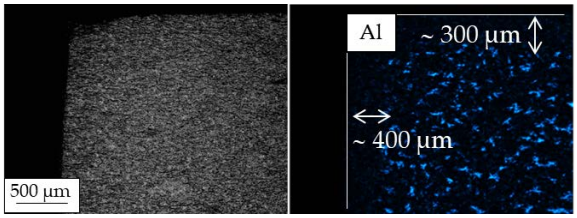

Fig. 12. EDS compositional map of the cross section of a sample sintered with 20 wt.% initial MCMB at 1900 °C for 30 h, where Al is highlighted in blue (primary electrons)

To discuss the different sintering behavior observed in samples with or without graphite sacrificial phase, the cross-section of the samples was analyzed by EDS. In figures 11 and 12, the compositional maps of the cross section of two samples are shown, with Al highlighted in blue; both samples were sintered with 20 wt.% initial MCMB. The presence of Al-rich clusters at the inner part of the samples can be noticed, appearing closer to the surface in the

sample sintered at higher temperature. EDS analysis of the Al-rich phases at higher magnifications are presented in figures 13 and 14; their high carbon content points to aluminum carbides as the possible composition.

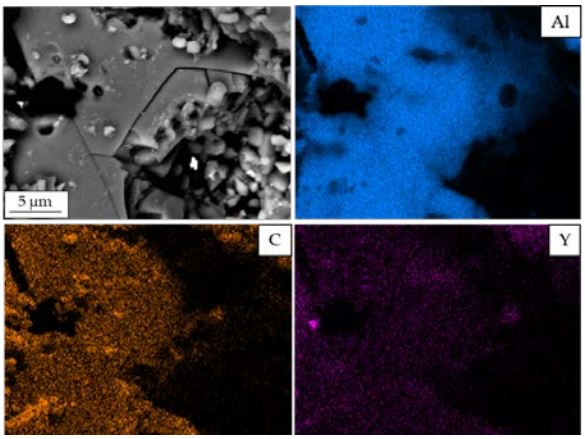

Fig. 13. Compositional maps of the Al-rich clusters at higher magnifications. Sample sintered with 20 wt.% initial MCMB at 1850 °C for 1 h (primary electrons)

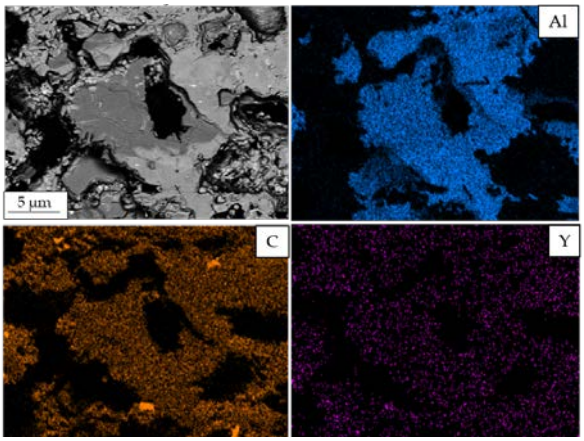

Fig. 14. Compositional maps of the Al-rich clusters at higher magnifications. Sample sintered with 20 wt.% initial MCMB at 1900 °C for 30 min (primary electrons)

In accordance with the processes described in the literature, in the present work it is suggested that liquid phases are formed by the interaction between the decomposition of SiC by Al_2O_3 and the free C present in the samples. If there is not enough open porosity in the material to allow the complete evaporation of these Al-C-Si products, their solidification during the cooling ramp may lead to the formation of the large Al-rich clusters, influenced by capillarity mechanisms allowed by the residual porosity present in the SiC matrix. The appearance of the Al-rich clusters can be then related to a combined effect between a high sintering temperature, the use of presureless sintering, and the presence of a high amount of C in the material during sintering. Besides, the possibility that the SiO_2 evaporation may be interacting with the above mechanisms, playing an active role in the formation and composition of the Al-rich phases, should be taken into consideration. More studies should be done focused on analyzing this possibility. The amount of open porosity present in the material in the different stages of sintering is an additional key factor determining the final microstructure of the material. No Al-rich clusters were detected in the final samples produced with 22 wt.% initial MCMB, both at 1850 °C or at 1900 °C. Even though a complete explanation cannot yet be provided with the data available, the considerably higher open porosity of this material after sintering may allow a more effective evaporation of the gaseous products during the last stages of the heating ramp, avoiding the formation of the Al-rich phases during cooling. An additional explanation to be explored is the possible oxidation and evaporation of the Al-rich carbides during the oxidation cycle due to the higher open porosity of these samples. Further analysis should be done in future works with samples produced with high amounts of MCMB.

The XRD diffraction patterns of the materials are shown in figures 15 and 16. A peak at 32.05° appears in those samples where the Al-rich clusters where observed more intensively in the microscopy analysis. Al_4C_3 and $Al_4C_7Si_4$ are proposed as possible phases, although it should be mentioned that their diffraction peaks (31.81 and 32.08° respectively) do not correspond exactly to the observed one.

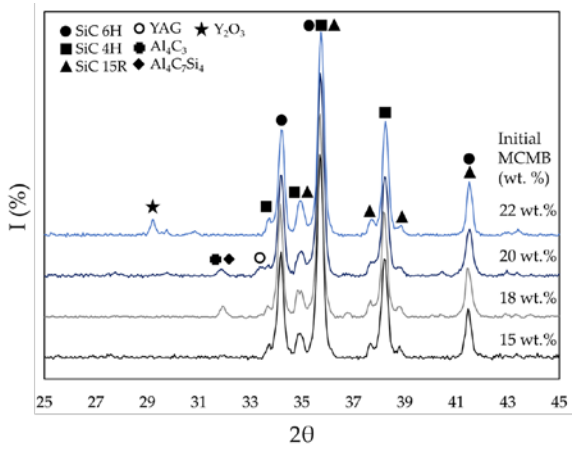

Fig. 15. X-ray diffraction patterns of the final samples produced with different initial MCMB content, sintered at 1850 °C for 1 h (after oxidation at 700 °C for 10 h). The thickness of the samples was reduced to analyze the composition of the internal Al-clusters

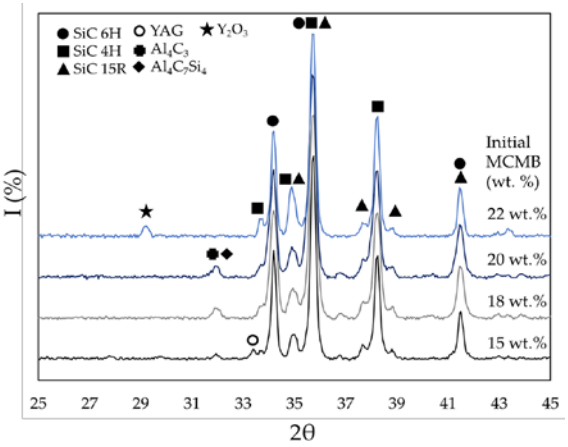

Fig. 16. X-ray diffraction patterns of the final samples produced with initial MCMB, sintered at 1900 °C for 30 min (after oxidation at 700 °C for 10 h). The thickness of the samples was reduced to analyze the composition of the internal Al-clusters

The main SiC polytypes in the final samples are the hexagonal 6H and 4H and the rhombohedral 15 R. The influence of liquid phases reacting with SiC in the sintering process is supported by the appearance of the phase SiC 15R, characterized by grains with high aspect ratio. The presence of phases derived from the Al_2O_3-Y_2O_3 phase diagram, like YAG, were detected only in small amount in some of the samples sintered in presence of MCMB. It is proposed that the interaction of the sintering additives with SiO_2 during the heating ramp, together with the formation of the Al-rich compounds, hinders the formation of phases derived from the Al_2O_3-Y_2O_3 interactions. In the samples with 22 wt.%, where the Al-rich clusters were not observed, a peak at 29.3° can be noticed. Y_2O_3 is suggested as a possible phase in this case, since the elimination of the initial Al_2O_3 during the sintering may inhibit its interaction with Y_2O_3 almost totally, remaining the initial amount of Y_2O_3 in the material.

5. Conclusions

- With the fabrication route proposed, i.e. by liquid phase sintering and using graphite spherical powder as sacrificial phase, high strength porous SiC materials with porosities in the range 35-50% were successfully fabricated.

- The influence of the initial SiC powder on the results obtained in the sintering was studied. Apart from aspects like the predominant polytypes or the particle size, the active role of the SiO_2 content was determined, as this phase interacts with the sintering additives during the heating ramp, forming liquid phases that promote densification and weight loss.

- The formation of an Al-Si liquid phase derived from the decomposition of SiC by Al_2O_3 at higher sintering temperatures, and its contribution to densification, is inhibited when graphite is used as sacrificial phase, since the formation of Al-rich carbides dominates over the formation of the metallic melt.

- The formation of phases derived from the Al_2O_3-Y_2O_3 combination that promote densification such as YAG, is hindered by the interaction of the sintering additives with SiO_2 and/or with SiC and graphite.

6. Acknowledgments

This work has been carried out within the framework of the EUROfusion Consortium and has received funding from the Euratom research and training programme 2014-2018 and 2019-2020 under grant agreement No 633053. The views and opinions expressed herein do not necessarily reflect those of the European Commission.

7. References

[1] K.A. Schwetz, Silicon carbide based hard materials, in: Handb. Ceram. Hard Mater., R. Riedel, Wiley-VCH, Weinheim, 2000: pp. 683–748.

[2] R.P. Jensen, W.E. Luecke, N.P. Padture, S.M. Wiederhorn, High-temperature properties of liquid-phase-sintered α-SiC, Mater. Sci. Eng. A. 282 (2000) 109–114. doi:10.1016/S0921-5093(99)00769-8.

[3] G.P. Kennedy, K.Y. Lim, Y.W. Kim, I.H. Song, H.D. Kim, Effect of SiC particle size on flexural strength of porous self-bonded SiC ceramics, Met. Mater. Int. 17 (2011) 599–605. doi:10.1007/s12540-011-0811-y.

[4] "CVD Silicon Carbide - DOW Chemical: https://www.dow.com/assets/attachments/business/gt/advanced_ceramics/cvd_silicon_carbide/tds/cvd_silicon_carbide.pdf.".

[5] J.-H. Eom, Y.-W. Kim, S. Raju, Processing and properties of macroporous silicon carbide ceramics: A review, J. Asian Ceram. Soc. 1 (2013) 220–242. doi:10.1016/j.jascer.2013.07.003.

[6] F. Wang, J. Yin, D. Yao, Y. Xia, K. Zuo, J. Xu, Fabrication of porous SiC ceramics through a modified gelcasting and solid state sintering, Mater. Sci. Eng. A. 654 (2016) 292–297. doi:10.1016/j.msea.2015.12.061.

[7] K. Raju, D.H. Yoon, Sintering additives for SiC based on the reactivity: A review, Ceram. Int. 42 (2016) 17947–17962. doi:10.1016/j.ceramint.2016.09.022.

[8] J. Zhang, D. Jiang, Q. Lin, Z. Chen, Z. Huang, Gelcasting and pressureless sintering of silicon carbide ceramics using Al2O3-Y2O3 as the sintering additives, J. Eur. Ceram. Soc. 33 (2013) 1695–1699. doi:10.1016/j.jeurceramsoc.2013.02.009.

[9] A. Kovalčíková, J. Dusza, P. Šajgalík, Thermal shock resistance and fracture toughness of liquid-phase-sintered SiC-based ceramics, J. Eur. Ceram. Soc. 29 (2009) 2387–2394. doi:10.1016/j.jeurceramsoc.2009.01.021.

[10] F.K. van Dijen, E. Mayer, Liquid phase sintering of silicon carbide, J. Eur. Ceram. Soc. 16 (1996) 413–420. doi:10.1016/0955-2219(95)00129-8.

[11] A. L. Ortiz, a. Munoz-Bernabé, O. Borrero-López, a. Domínguez-Rodríguez, F. Guiberteau, N.P. Padture, Effect of sintering atmosphere on the mechanical properties of liquid-phase-sintered SiC, J. Eur. Ceram. Soc. 24 (2004) 3245–3249. doi:10.1016/j.jeurceramsoc.2003.10.047.

[12] E. Gomez, J. Echeberria, I. Iturriza, F. Castro, Liquid phase sintering of SiC with additions of Y2O3, Al2O3 and SiO2, J. Eur. Ceram. Soc. 24 (2004) 2895–2903. doi:10.1016/j.jeurceramsoc.2003.09.002.

[13] C. Soto, C. Garcia-Rosales, J. Echeberria, E. Platacis, A. Shisko, F. Muktepavela, T. Hernandez, M.M. Huertac, Development, Characterization, and Testing of a SiC-Based Material for Flow Channel Inserts in High-Temperature DCLL Blankets, IEEE Trans. Plasma Sci. (2018). doi:10.1109/TPS.2018.2809571.

[14] M. Malo, C. Soto, C. García-Rosales, T. Hernández, Stability of porous SiC based materials under relevant conditions of radiation and temperature, J. Nucl. Mater. 509 (2018) 54–61. doi:10.1016/j.jnucmat.2018.06.009.

[15] C. Soto, Development of a SiC-based material for Flow Channel Inserts in high-temperature DCLL blankets, PhD thesis, Universidad de Navarra, 2018.

[16] T. Grande, H. Sommerset, E. Hagen, K. Wiik, M. a Einarsrud, Effect of Weight Loss on Liquid-Phase-Sintered Silicon Carbide, J. Am. Ceram. Soc. 80 (1997) 1047–1052. doi:10.1111/j.1151-2916.1997.tb02945.x.

[17] J. Eom, Y. Kim, Effect of template size on microstructure and strength of porous silicon carbide ceramics, J. Ceram. Soc. Japan. 10 (2008) 1159–1163. doi:10.2109/jcersj2.116.1159.

[18] S.-H. Chae, Y.-W. Kim, I.-H. Song, H.-D. Kim, M. Narisawa, Porosity control of porous silicon carbide ceramics, J. Eur. Ceram. Soc. 29 (2009) 2867–2872. doi:10.1016/j.jeurceramsoc.2009.03.027.

[19] G.-D. Zhan, M. Mitomo, Microstructural control for strengthening of silicon carbide ceramics, J. Am. Ceram. Soc. 82 (1999) 2924. doi:10.1111/j.1151-2916.1999.tb02181.x.

[20] H. Xu, T. Bhatia, S.A. Deshpande, N.P. Padture, A.L. Ortiz, F.L. Cumbrera, Microstructural Evolution in Liquid-Phase-Sintered SiC: Part I, Effect of Starting Powder, J. Am. Ceram. Soc. 84 (2001) 1578–1584. doi:10.1111/j.1151-2916.2001.tb00880.x.

[21] J.-H. Eom, Y.-W. Kim, Effect of initial α-phase content on microstructure and flexural strength of macroporous silicon carbide ceramics, Met. Mater. Int. 18 (2012) 379–383. doi:10.1007/s12540-012-2025-3.

[22] A. Can, M. Herrmann, D.S. McLachlan, I. Sigalas, J. Adler, Densification of liquid phase sintered silicon carbide, J. Eur. Ceram. Soc. 26 (2006) 1707–1713. doi:10.1016/j.jeurceramsoc.2005.03.253.

[23] L. Stobierski, A. Gubernat, Sintering of silicon carbideI. Effect of carbon, Ceram. Int. 29 (2003) 287–292. doi:10.1016/S0272-8842(02)00117-7.

[24] A. Bereciartu, "Manufacturing of porous SiC with dense SiC layer for application as Flow Channel Inserts in future nuclear fusion reactors", PhD thesis, Universidad de Navarra, 2014.

[25] A.K. Misra, Thermochemical Analysis of the Silicon Carbide-Alumina Reaction with Reference to liquid-Phase Sintering of Silicon Carbide, 51 (1991) 345–351.

[26] J. Ihle, M. Herrmann, J. Adler, Phase formation in porous liquid phase sintered silicon carbide: Part II: Interaction between Y2O3 and SiC, J. Eur. Ceram. Soc. 25 (2005) 997–1003. doi:10.1016/j.jeurceramsoc.2004.04.016.

[27] S. Baud, F. Thevenot, A. Pisch, C. Chatillon, High temperature sintering of SiC with oxide additives: I. Analysis in the SiC-Al2O3 and SiC-Al2O3-Y2O3 systems, J. Eur. Ceram. Soc. 23 (2003) 1–8. doi:10.1016/S0955-2219(02)00067-5.

[28] J. Ihle, M. Herrmann, J. Adler, Phase formation in porous liquid phase sintered silicon carbide: Part I: Interaction between Al2O3 and SiC, J. Eur. Ceram. Soc. 25 (2005) 987–995. doi:10.1016/j.jeurceramsoc.2004.04.015.

[29] R. Neher, M. Herrmann, K. Brandt, K. Jaenicke-Roessler, Z. Pan, O. Fabrichnaya, H.J. Seifert, Liquid phase formation in the system SiC, Al2O3, Y2O3, J. Eur. Ceram. Soc. 31 (2011) 175–181. doi:10.1016/j.jeurceramsoc.2010.09.002.